TECHNICAL PAPER

ISSN:1047-3289 *J. Air & Waste Manage. Assoc.* **61**:418–426
DOI:10.3155/1047-3289.61.4.418


# Heterogeneous Mercury Reaction Chemistry on Activated Carbon

**Jennifer Wilcox, Erdem Sasmaz, and Abby Kirchofer**
*Department of Energy Resources Engineering, School of Earth Sciences, Stanford University, Stanford, CA*

**Sang-Sup Lee**
*Department of Environmental Engineering, Chungbuk National University, Cheongju, South Korea*

## ABSTRACT
Experimental and theory-based investigations have been carried out on the oxidation and adsorption mechanism of mercury (Hg) on brominated activated carbon (AC). Air containing parts per billion concentrations of Hg was passed over a packed-bed reactor with varying sorbent materials at 140 and 30 °C. Through X-ray photoelectron spectroscopy surface characterization studies it was found that Hg adsorption is primarily associated with bromine (Br) on the surface, but that it may be possible for surface-bound oxygen (O) to play a role in determining the stability of adsorbed Hg. In addition to surface characterization experiments, the interaction of Hg with brominated AC was studied using plane-wave density functional theory. Various configurations of hydrogen, O, Br, and Hg on the zigzag edge sites of graphene were investigated, and although Hg-Br complexes were found to be stable on the surface, the most stable configurations found were those with Hg adjacent to O. The Hg-carbon (C) bond length ranged from 2.26 to 2.34 Å and is approximately 0.1 Å shorter when O is a nearest-neighbor atom rather than a next-nearest neighbor, resulting in increased stability of the given configuration and overall tighter Hg-C binding. Through a density of states analysis, Hg was found to gain electron density in the six p-states after adsorption and was found to donate electron density from the five s-states, thereby leading to an oxidized surface-bound Hg complex.

## INTRODUCTION
Because of mercury (Hg) amalgam use or replacement, elemental mercury ($Hg^0$) vapor concentrations of up to approximately 27 $\mu g/m^3$ in the air of dental offices have been documented.[1,2] Several neuropsychological studies over the last 29 yr have investigated an increase in symptoms of cognitive malfunction and impairment within dental personnel and dentists.[3–9] When $Hg^0$ is inhaled, it is transported throughout the body via the bloodstream and can pass through the blood-brain barrier, subsequently oxidizing to $Hg^{2+}$.[10] Functionalized activated carbon (AC) may be a suitable sorbent for Hg removal for this application. Understanding the mechanisms associated with sorbent functionalization for enhanced $Hg^0$ uptake in air and at ambient conditions is required to make this a viable option. Previous experimental studies[11] involving carbon (C) sorbents for the oxidation and/or adsorption of $Hg^0$ have been primarily focused on the application of capture from coal-fired power plant emissions, which are far more complex than the air investigations of the work presented here. However, knowledge and brief review of what has been learned within this related application will provide insight into the chemical mechanisms by which functionalized C sorbents act to effectively adsorb metallic Hg and its oxidized forms.

Huggins et al.[12,13] investigated various C samples exposed to Hg at simulated coal combustion flue gas conditions and characterized them using X-ray absorption fine structure (XAFS) spectroscopy. The XAFS spectra provided strong indication of Hg chemisorption on C. Their data suggest that the adsorption process occurs through a combination of halide, sulfide, and oxygen anions (either C-bound or C-sulfate-bound) present on the C surface. Additionally, Hutson et al.[14] characterized chlorinated and brominated AC using X-ray absorption spectroscopy and X-ray photoelectron spectroscopy (XPS) after exposing the carbons to simulated flue gas containing $Hg^0$ (204 $\mu g/m^3$; 24 parts per billion by volume [ppbv]). They found no $Hg^0$ on the AC surface, but they found adsorbed Hg-bromine (Br) and Hg-chlorine (Cl) complexes and propose that Hg capture by chlorinated and brominated carbons is achieved by surface oxidation of $Hg^0$ with subsequent adsorption. Finally, Laumb et al.[15] have carried out surface analyses on ACs exposed to Hg-doped simulated flue gas, but they were unable to determine conclusively the oxidative state of surface-bound Hg because of XPS-measured interference with silicon (Si), which is present at comparable levels to Hg within the C matrix.

The work presented here involves the investigation of the possible binding mechanism of Hg on AC sorbents

### IMPLICATIONS
The design of Hg capture sorbents from air has application to Hg removal from dentist offices because of the elevated elemental mercury vapor concentrations in these environments from amalgam use or replacement. This work serves as the foundation for potential optimization of AC's properties to make this capture technology more effective and potentially less costly.

through packed-bed experiments, experimental characterization, and electronic structure calculations. Surface characterization experiments using XPS were carried out before and after exposure to air containing $Hg^0$ (203–10,817 $\mu g/m^3$; 24–1296 ppbv), which is crucial for determining the form of surface-bound Hg. Although the concentrations in air for the application of interest in the work presented here are lower than 200 $\mu g/m^3$, these elevated levels were investigated to obtain sufficient surface concentrations of Hg for detection using XPS. It is assumed that at these low concentrations the mechanism of oxidation and/or adsorption would not differ substantially. The difference would be a potential increase in the Hg-Hg interactions taking place. Unfortunately, because mercury oxide (HgO), mercury bromide ($Hg_2Br_2$), and mercury bromide ($HgBr_2$) have similar binding energies in XPS, these surface-bound species will not be speciated. To further assist in determining the mechanism by which $Hg^0$ oxidizes and subsequently adsorbs on functionalized C, electronic structure calculations based on plane-wave density functional theory (DFT) have been carried out to determine the surface reactivity and subsequent stability of surface-bound Hg species.

## OVERVIEW

### Experimental Methods

Hg-adsorbed C samples have been prepared to identify the species of Hg adsorbed on C surfaces using XPS to investigate the possible Hg binding mechanisms. A packed-bed reactor system was constructed as shown in Figure 1 to prepare the samples in an air environment containing $Hg^0$. The powdered AC (e.g., 20 mg) samples were placed in a 1.27 cm-diameter quartz packed-bed reactor. The reactor is covered with a 50-cm-long ceramic fiber heater (Semi-Cylindrical Units-Embedded Coiled Elements, Watlow) to conduct tests at controlled temperatures and to obtain a uniform temperature profile in the reactor. $Hg^0$ vapor is introduced from an Hg calibration system (PSA 10.536 Mercury Calibration System, PS Analytical) and the outlet flow is measured using a commercially available Hg analyzer (PSA 10.525 Sir Galahad System, PS Analytical). The results described here are based on pure $Hg^0$ injection with air over commercially available brominated AC (DARCO Hg-LH) and nonbrominated AC (DARCO Hg) sorbents, which are available through NORIT Americas, Inc. Various conditions were considered: (1) 140 °C, 203 $\mu g/m^3$ (24 ppbv, STD), with a flow rate of 2 L/min; (2) 140 °C, 6761 $\mu g/m^3$ (810 ppbv, STD), with a flow rate of 0.5 L/min; and (3) 30 °C, 10,817 $\mu g/m^3$ (1296 ppbv, STD), with a flow rate of 0.5 L/min. These packed-bed tests were conducted until breakthrough was achieved (i.e., when the outlet $Hg^0$ concentration approached the inlet $Hg^0$ concentration). Because of the inherent Si-containing nature of AC, there was interference of oxidized Hg compounds and Si because of the similarity in their electron binding energies. To use XPS for surface characterization of Hg on C, it was necessary to investigate lower temperature conditions to increase Hg adsorption capacity of the C sorbent and to maximize the amount of Hg adsorbed on the sorbent surface. It is assumed that the chemical and related electronic interaction between Hg and the edge-site atoms would be the same at lower temperatures.

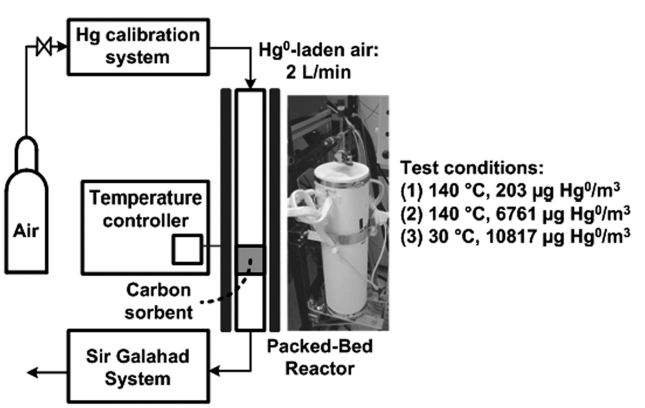


**Figure 1.** Schematic of the packed-bed reactor system.

The sorbent surface is oxidizing and adsorbing. A question is whether the oxidation step proceeds via an Eley–Rideal mechanism, by which Hg strikes an adsorbed Br atom with the collision leading to oxidized Hg, or whether oxidation occurs via a Langmuir–Hinshelwood mechanism by which Hg strikes the surface, adsorbs, and reacts on the surface with a Br atom to form oxidized Hg. In both cases, the product formed will remain on the surface as an adsorbed complex or desorb directly into the gas phase, completing the reaction process. This step will depend on the relative stability of the reaction intermediates on the surface and the temperature and pressure conditions of the system. For instance, adsorption is an exothermic process so that a higher temperature would lead to desorption and in a similar manner, a decreased pressure would also lead to desorption. The Eley–Rideal mechanism requires that a reaction is barrierless and exothermic.[16] If a barrier to Hg oxidation exists, then the reaction pathway likely proceeds via a Langmuir–Hinshelwood mechanism. Previous investigations have shown that in the case of radical hydrogen (H) interactions with halogenated surfaces (gold[17,18] and Si[19]), the mechanism proceeds via an Eley–Rideal mechanism. Because $Hg^0$ is not expected to be in radical form at the temperature and pressure conditions of the work presented here, it is the authors' hypothesis that Hg oxidation proceeds via a Langmuir–Hinshelwood mechanism. In particular, the thermal energy of the system at 140 °C is only 0.818 kcal/mol and 0.600 kcal/mol at 30 °C. To test this hypothesis, XPS experiments were carried out on C samples before and after exposure to $Hg^0$.

The XPS experiments were performed using a Physical Electronics (PHI) 5000VersaProbe scanning XPS system at the Stanford Nanocharacterization Laboratory at Stanford University. The data reduction was carried out with PHI MultiPak Software. The instrument is not equipped with a cold stage and the vacuum is $10^{-11}$ Torr, implying that physisorbed Hg ($Hg^0$) will likely be removed from the surface under the transport and analysis of the sample and that the observed surface-bound Hg was likely strongly adsorbed. Spectra were collected using monochromatic Al Kα radiation at 1486 eV.

### Theoretical Methods

Electronic structure calculations were carried out using plane-wave DFT to determine the surface reactivity of AC

to Hg and surface-bound oxidized Hg species. DFT calculations were carried out using the Vienna Ab Initio Simulation Package.[20,21] The projector augmented wave method was used to describe the ion-electron interactions.[22,23] Electron exchange-correlation functionals are represented with the generalized gradient approximation, and the model of Perdew, Burke, and Ernzerhof is used for the nonlocal corrections.[24] The energy cutoff for the plane wave expansion was 400 eV, and Methfessel and Paxton Gaussian smearing of order 1 was used with a width of 0.2 eV to accelerate convergence of the total energy calculations.[25] The surface Brillouin zone integration was calculated using a γ-centered $5 \times 5 \times 1$ (for slab) or $5 \times 1 \times 1$ (for ribbon) Monkhorst–Pack mesh.[26] Geometric optimization was performed using the conjugate-gradient algorithm until the absolute value of the forces on unconstrained atoms was less than 0.03 eV/Å.

The partial density of states (DOS) were calculated by projecting the electronic wave functions onto spherical harmonics centered on Hg, oxygen (O), and Br atoms. The integral of the DOS up to the Fermi level is proportional to the number of electrons participating in bonding and local reactivity. In general, the DOS analysis allows for an understanding of how electrons are covalently shared between different atoms. In this work, the DOS analysis of the s- and p-states of the simulated AC and the states of the surface-bound atoms (O and Br) have been investigated along with the s-, p-, and d-states of surface-bound Hg to determine the mechanism associated with Hg binding to C.

## RESULTS AND DISCUSSION

### Surface Characterization of AC

Packed-bed reactor experiments were carried out to determine $Hg^0$ oxidation and binding mechanisms in an air environment. It was found that the use of sand and quartz wool in the packed-bed tests should be limited because their composition includes Si, which interferes with the oxidized Hg XPS spectra; therefore, the experiments presented here were carried out in the absence of sand to isolate the Hg spectra. However, through an XPS survey scan the AC was found to inherently contain 0.8 and 1.3 atom % Si for the brominated and nonbrominated AC, respectively. This concentration was still higher than that of Hg present on the sorbent. Specifically, the Si 2p and Hg 4f peaks interfere with each other in the binding region between 100.7 and 104 eV, which is the region where oxidized species such as $HgBr_2$, $Hg_2Br_2$, and HgO would be located. To circumvent these challenges, a higher concentration of $Hg^0$ was used in the gas stream passing through the packed bed (1296 ppbv). Additionally, for XPS detection the sorbent experiments were carried out at lower temperatures to maximize adsorption, which is an exothermic process. The XPS survey scan of the sorbent reveals that the brominated AC contains 15.8% O and 0.4% Br, whereas the nonbrominated AC contains only O at 14.2%. It is important to note that XPS is a surface-sensitive technique and that these levels of Br detected are comprised of the Br available at the surface for interacting with $Hg^0$. A technique such as inductively coupled mass spectrometry could be used to determine the total Br content of the sample, but this was beyond the scope of this study. Additionally, some of the potentially physisorbed Br contained in the sample may have been removed upon exposure to the ultrahigh vacuum environment of the XPS instrument.

Determining the speciation among the various surface-bound oxidized Hg species is difficult using XPS. The $4f_{7/2}$ binding energies of Hg compounds ($Hg^0$, HgO, $HgBr_2$, $Hg_2Br_2$) range from 99.9 eV ($Hg^0$) to 101.0 eV ($HgBr_2$). The Hg 4f core level XPS spectra for Hg-containing AC sorbents are shown in Figure 2 for various conditions. The interference of Si is visible in Figures 2a–2c and clearly masks the Hg peaks. Increasing the gas-phase $Hg^0$ concentration to 10,817 μg/m$^3$ (1296 ppbv) reveals the two distinguishing oxidized Hg $4f_{5/2}$ and $4f_{7/2}$ peaks in Figure 2b centered around 104.53 and 100.59 eV, respectively. From Figure 2, a and c, it can be seen that with increasing the gas-phase Hg concentration from 203 (24 ppbv) to 6761 μg/m$^3$ (810 ppbv), the Hg doublet is just slightly enhanced in the latter; however, because of the noise in the data, additional characterization experiments should be carried out to verify this slight observed increase. It should be noted that the absolute intensities of the XPS spectra do not carry a lot of meaning, but rather the relative intensities within a given spectrum do. The reason that relative rather than absolute intensities carry the meaning is that there are aspects of the measurement (e.g., source produces more X-rays one day vs. another, height of one sample is 100 μm higher than another, etc.) that can change from day to day. This is why the baseline-untested data in Figures 2a–2d each differ from one another.

Table 1 provides a summary of the XPS Hg and Br binding energies for Hg-Br reference compounds available in the literature[27] and for the Hg-containing brominated AC sorbent investigated in the work presented here compared with the study carried out by Hutson et al.[14] The reference data for the Hg $4f_{7/2}$ binding energy of $HgBr_2$ indicate that this is the primary form of oxidized Hg on the surface; however, reference data are not available for the Hg $4f_{5/2}$ binding energy for this compound. Additionally, reference data are not available for a potentially surface-bound species of HgBr with an oxidation state of +1. To determine the speciation of the Hg doublet in Figure 2d, the reference data were compared. According to Table 1, the HgO doublet reference is 104.78 and 100.8 eV, compared with the measured doublet of 104.53 and 100.59 eV. This would imply that the doublet is HgO; however, when testing nonbrominated AC as shown in Figure 2d, it would be expected that the same doublet would be seen if Br in fact did not play the role in oxidation. Another option is a required combination of Br and O for Hg oxidation to take place. Further analysis of the Hg $4f_{7/2}$ reference peaks in Table 1 indicate that the doublet may belong to HgO, $Hg_2Br_2$, or $HgBr_2$ because the binding energies for these are 100.8, 100.7, and 101.0 eV, respectively, compared with that of 100.59 eV in the work presented here. It is also important to note that these results compare quite well to those of Hutson et al.[14] Also, from the XPS scan it was found that there was approximately 40 times more O than Br within the sorbent sampled, implying that if both of these species are

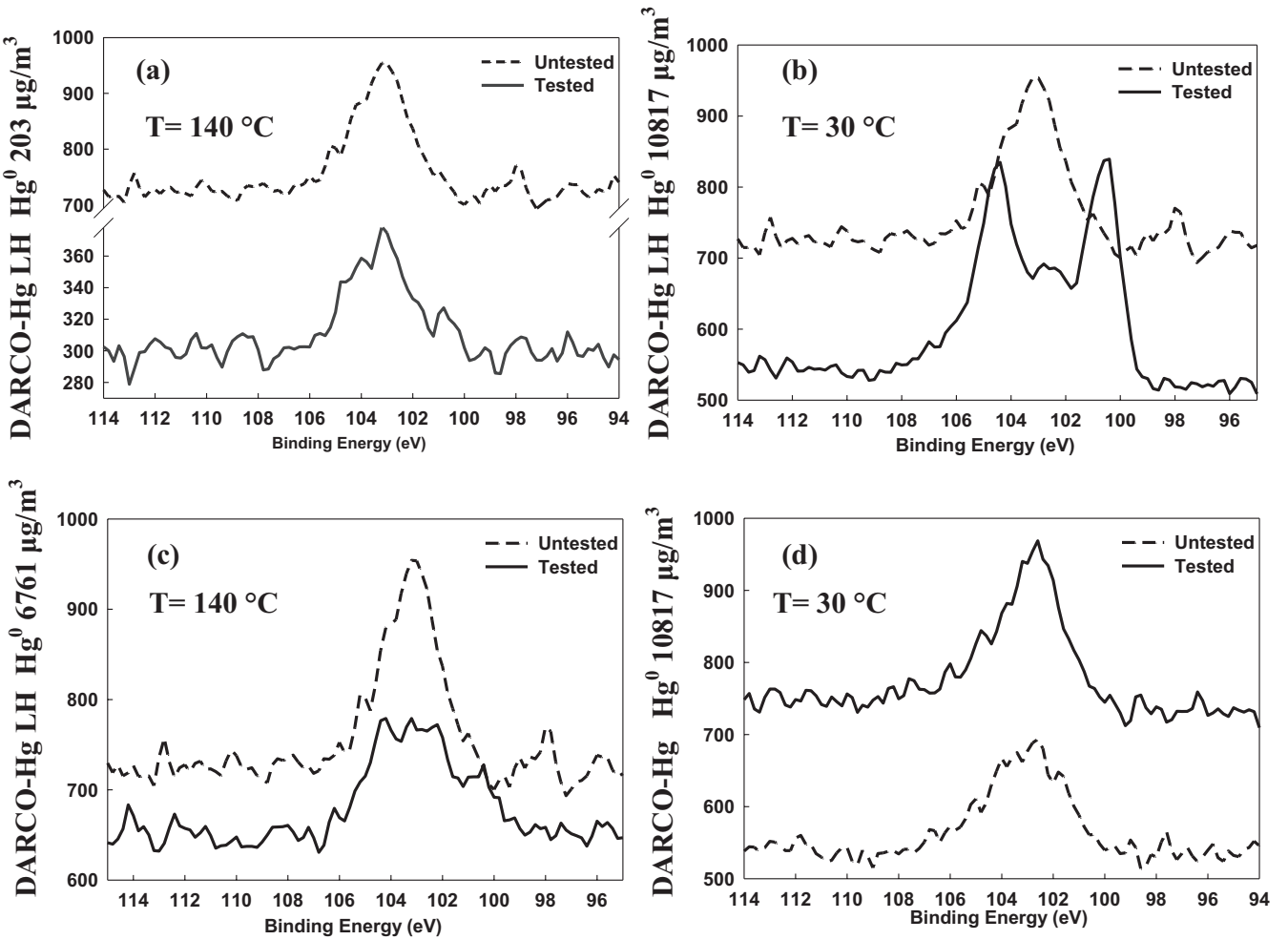


**Figure 2.** Hg 4f core level XPS spectra for AC sorbents at various indicated conditions: (a–c) Br-AC sorbents and (d) virgin-AC sorbent.

reactive, and if $Hg^0$ has the potential to "see" O more often than Br, then the HgO doublet should be more prevalent in the XPS spectra. Although the O is present to a higher extent, its availability to bind is questionable. In other words, without a more detailed analysis of the differences in how O and Br are each coordinated within the pore surfaces or bulk matrix of the C, it is difficult to infer what percent of the O is actually available to interact with $Hg^0$. At the elevated concentration and low temperature, the doublet peak of oxidized Hg is clearly evident in Figure 2b, with the oxidized form currently unknown. It is also clear from this figure that the doublet of $Hg^0$ is not present at 99.9 and 104.0 eV.

**Table 1.** XPS binding energies for $Hg^0$, Hg-Br, and HgO: References and Hg-containing brominated AC.

| | Hg $4f_{5/2}$ | Hg $4f_{7/2}$ | ΔE (eV) | Br $3d_{5/2}$ |
|---|---|---|---|---|
| Reference[27] | | | | |
| $Hg^0$ | 104.0 | 99.9 | 4.1 | – |
| $HgBr_2$ | – | 101.0 | – | 69.3 |
| $Hg_2Br_2$ | – | 100.7 | – | 69.8 |
| HgO | 104.78 | 100.8 | 3.98 | – |
| Hutson et al.[14] | | | | |
| DARCO Hg-LH | 105.3 | 101.4 | 3.9 | 69.7 |
| This study | | | | |
| DARCO Hg-LH | 104.53 | 100.59 | 3.94 | 69.0 |

The evidence of these results implies that Hg adsorption at this low temperature and elevated concentration involves a chemical reaction, which, as outlined previously, would have an activation barrier if it were to proceed via a Langmuir–Hinshelwood mechanism. As a result, it appears that the data indicate one of the following:

- The oxidation reaction proceeds via an Eley–Rideal mechanism.
- The oxidation reaction proceeds via a Langmuir–Hinshelwood reaction with the activation barrier being overcome because of a cooperative effect based on high Hg coverage or Hg-Hg interactions due to the increased concentration.
- There is a two-step adsorption process in which Hg is first oxidized by Br via one of the two mechanisms as previously described, desorbs from the surface into the gas phase, and readsorbs to the surface.

The difference between the roles of O and Br with regards to Hg capture was further investigated in this study through electronic structure calculations, which allow for deeper probing into the chemical bonding and potential surface complexes formed by these three species on C surfaces.

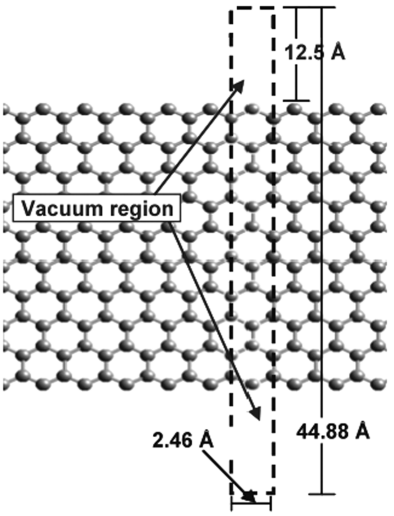


**Figure 3.** Computational domain of model C ribbon with exposed zigzag edge sites.

### Electronic Structure of Hg-Bound C

AC is exceedingly difficult to model given its highly inhomogeneous structure. Graphene may be used as a simplified model of carbonaceous surfaces to study the reactivity of sorbents such as AC.[28] The model of a single layer of graphene with unsaturated edge atoms to create active sites has been used in multiple studies to simulate carbonaceous surfaces.[29–32] Previous studies have considered models of C edges comprised of armchair and zigzag sites.[33–36] The major conclusion from these previous investigations is that the zigzag sites with carbene atoms are the most reactive with the C atom having two unpaired electrons.[37,38] The goal of this work is to identify trends in the adsorption and oxidation of $Hg^0$ on functionalized edge sites under relevant conditions of the surrounding flue gas. To model Hg adsorption on brominated, oxygenated, or hydrogenated C edge sites, a realistic model of the C sorbent and, specifically, its potential reaction sites, must be defined.

The parameters used for the electronic structure calculations are first benchmarked by comparing C-C bond distances predicted by theory against experiments through simulating a bulk two-dimensional graphene sheet. Because the computational domain is periodic in three dimensions, the sheet is isolated from its periodic image sheets by a 10-Å vacuum region. The optimized C-C bond length of 1.42 Å is in perfect agreement with the experimental results of 1.42 Å.[39–41] Because halogens (in particular, Cl and Br) and Hg have been found to react with the zigzag edge sites of graphene, the initial investigations use a graphene sheet with zigzag edge sites to model the reactive C surface.[42] The "surface" edge sites of the graphene sheet are created by modeling a slice perpendicular to the two-dimensional basal plane. A 25-Å vacuum is then used to isolate the edge sites from their periodic images. Two surfaces are required to correctly resolve the surface dipole layers. The result is shown in Figure 3, with the two surfaces separated by 20 C atom layers, or 9 hexagonal C "rings," in which each ring consists of 4 layers of C atoms. The atoms outlined in the figure are the atoms included in the computational domain. The nine layers of rings were found to be the minimum necessary to ensure that the surfaces do not interact and that the center region retains the bulk configuration. Testing was carried out to determine the minimum number of C rings. C ribbons were simulated with depths ranging from 3 to 31 rings, and the change in C-C bond distance was recorded as a function of distance from the surface.

The change in the C-C bonds during energy optimization is quantified by the percent relaxation of the C-C bonds from the bond distance represented in a bulk graphene system. As the number of layers was increased, the two symmetric edges, shown in Figure 3, interacted less, resulting in a decrease in relaxation (i.e., change from C-C bond distance of the bulk system). As the number of rings used to represent graphene was increased, the relaxation of the surface bonds converged to ±2% with no relaxation or bond-distance change within the center atoms. On the basis of these investigations, a graphene ribbon nine rings deep was determined to be the appropriate size to model the zigzag edge sites of AC. Using the nine-ring-deep graphene ribbon model, electronic structure calculations were carried out to determine the most stable concentrations and configurations of H, Br, O, and Hg atoms at the edge sites. The initial investigations are represented with edges that contain five sites on each side of the graphene ribbon. Each structure is labeled in the form "X-X-X-X-X," where the five letters represent the surface coverage of the five zigzag edge sites of graphene. The sampled coverages include various combinations of O, H, Br, and Hg bound at an edge site. Within this initial investigation, the number and type of atom is consistent with the neighbor and nearest-neighbor configurations tested to determine which configuration results in the more stable edge. Although six configurations were tested overall, the two lowest and one highest configuration are adequate to discuss the trends in reactivity observed. These three configurations are pictured in Figure 4. Each atom—Hg, O, H, and Br—is covalently bonded to the surface C edge site, but each also interacts to a certain extent with their nearest and next-nearest neighbor on neighboring edge sites, with

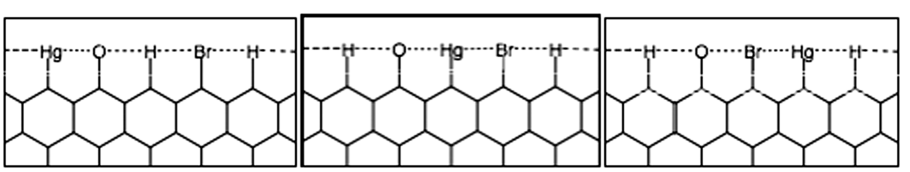


**Figure 4.** Surface configurations analyzed in the work presented here with stabilities ranging from the left (−945.113 eV) and center (−944.471 eV) to the right (−943.773 eV), with the configuration on the left being the most stable.

**Table 2.** Energies and bond distances of tested edge-site configurations.

| Structure | DFT Energy (eV) | Hg-C Distance (Å) | Br-C Distance (Å) | O-C Distance (Å) | Br-O Distance (Å) | Hg-O Distance (Å) | Hg-Br Distance (Å) |
|---|---|---|---|---|---|---|---|
| Hg-O-H-Br-H | −945.113 | 2.26 | 1.90 | 1.25 | – | 2.63 | – |
| H-O-H-Br-Hg | −944.474 | 2.32 | 1.91 | 1.24 | – | – | 3.01 |
| H-O-Hg-Br-H | −944.471 | 2.27 | 1.92 | 1.25 | – | 2.49 | 2.99 |
| Hg-O-Br-H-H | −944.417 | 2.27 | 1.90 | 1.25 | 2.74 | 2.61 | – |
| H-O-Br-H-Hg | −944.259 | 2.32 | 1.90 | 1.24 | 2.77 | – | – |
| H-O-Br-Hg-H | −943.773 | 2.34 | 1.91 | 1.24 | 2.66 | – | 2.92 |

the interaction indicated in Figure 4 through a dotted line between the edge-site atoms.

Table 2 provides the energy of each of the system configurations tested and the bond length between the bound Hg and the surface C atom. To the authors' knowledge, the Hg-C bond length for Hg adsorbed on graphene has not been experimentally determined; however, the Hg-C bond length for various Hg-organic complexes has been determined and ranges from 2.21 Å in $Hg(C_6F_5)(CH_2CH_2PPH_2)_3(CF_3SO_3)$[43] to 2.35 Å when Hg is bonded para to a toluene methyl group.[44] The Hg-C bond lengths calculated in this investigation (2.26–2.34 Å) agree reasonably well with the Hg-C bond lengths in other Hg-organic complexes, but experimental work on Hg-graphene to determine the Hg-C bond length is needed for comparison.

The interaction distances suggest that Hg and Br tend to repel each other while interacting closer to an H or O neighbor if such an opportunity exists. For instance, the Hg-O distances in Hg-O-H-Br-H (2.63 Å) and Hg-O-Br-H-H (2.61 Å) configurations, in which Hg is not adjacent to Br, are greater than in the H-O-Hg-Br-H (2.49 Å) configuration, in which Hg is adjacent to Br, suggesting that Hg repels away from Br toward O, thereby decreasing the Hg-O bond distance. Similarly, the Br-O distances in Hg-O-Br-H-H (2.74 Å) and H-O-Br-H-Hg (2.77 Å) configurations, in which Br is not adjacent to Hg, are greater than in the H-O-Br-Hg-H (2.66 Å) configuration, in which Br is adjacent to Hg.

By comparing the Hg-C bond lengths of the various structures, the significance of the surface atom configuration on the Hg-graphene interaction is also evident. For instance, the Hg-C bond length corresponds highly to the proximity of Hg to O. Specifically, in structures with a surface atom configuration that includes Hg-O, the Hg-C bond lengths are 2.26Å (Hg-O-H-Br-H) or 2.27Å (H-O-Hg-Br-H and Hg-O-Br-H-H); for the structure with Hg and O separated by a H atom, the Hg-C bond distances are 2.32 Å (H-O-H-Br-Hg and H-O-Br-H-Hg) and 2.34 Å(H-O-Br-Hg-H). In summary, the graphene surface C atom binds to Hg more tightly when the neighboring surface atom is O, and the Hg-graphene structure is most stable when Hg is located next to a surface O atom but not immediately next to a bound Br atom.

From these results there appears to be some lateral interaction that increases the binding strength of Hg when the neighboring atom is O but decreases the strength when the interaction is with a Br atom. To further investigate these relationships, a DOS analysis was undertaken for the three structures in Figure 4. The Hg s-, p-, and d-DOS before and after adsorption on the H-O-Hg-Br-H, Hg-O-H-Br-H, and H-O-Br-Hg-H edges are shown in Figures 5a–5c, respectively. The s-, p-, and d-states of the Hg atom change appreciably after adsorption, signifying the strong interaction with the surface.

In particular, it can be seen that before adsorption no electrons are found in the 6 p-states of Hg, but after Hg interacts with the surface, there is an increase in electron density in these states. In regard to the d-states, although the peak shape has not changed, the energy has been reduced, denoting an additional interaction with the surface. The most information about the Hg-surface interaction, and in particular the differences between the interactions with the various surface configurations, is found in the DOS of the s-states of Hg. As can be seen in Figure 5a, not only does the shape of the DOS change after adsorption, but there is also a marked difference between the s-states of the lowest-energy Hg-O-H-Br-H surface and the other two surfaces. When Hg is in the Hg-O-H-Br-H configuration, there is a single main peak at approximately −3.5 eV and a smaller one at approximately −1.9 eV. In comparison, when Hg is in either of the other two configurations (i.e., H-O-Hg-Br-H and H-O-Br-Hg-H), the electron density is distributed into two or more main peaks. A wide distribution of states generally indicates a weakening of the overall interaction, which appears to be happening in these two cases.

To further understand the mechanism affecting the interaction, the DOS of the s-, p-, and d-states of all of the surface atoms were plotted and are shown in Figure 6 for H-O-Hg-Br-H (Figure 6a), Hg-O-H-Br-H (Figure 6b), and H-O-Br-Hg-H (Figure 6c). Because of the differences in magnitude, the s- and p-orbitals are plotted on a smaller scale (left axis) than the d-orbitals (right axis).

The plots in Figure 6 provide information regarding the correlation of surface-bound Hg with the other surface atoms and show that the surface atom interactions change significantly depending on the surface atom configuration. In Figure 6c (H-O-Br-Hg-H, in which Br and O are adjacent), the Br and O p-orbitals are strongly correlated at −1.0 and −2.4 eV. This strong Br-O interaction is not present in the Hg-O-H-Br-H configuration, in which H separates O and Br; however, a similar strong correlation between the Br and O p-orbitals is shown in Figure 6a (H-O-Hg-Br-H), suggesting that Hg serves to bridge O and Br, forming a triatomic complex at the surface.

Surface-bound Br influences the interaction between Hg and the C by modifying the electron density

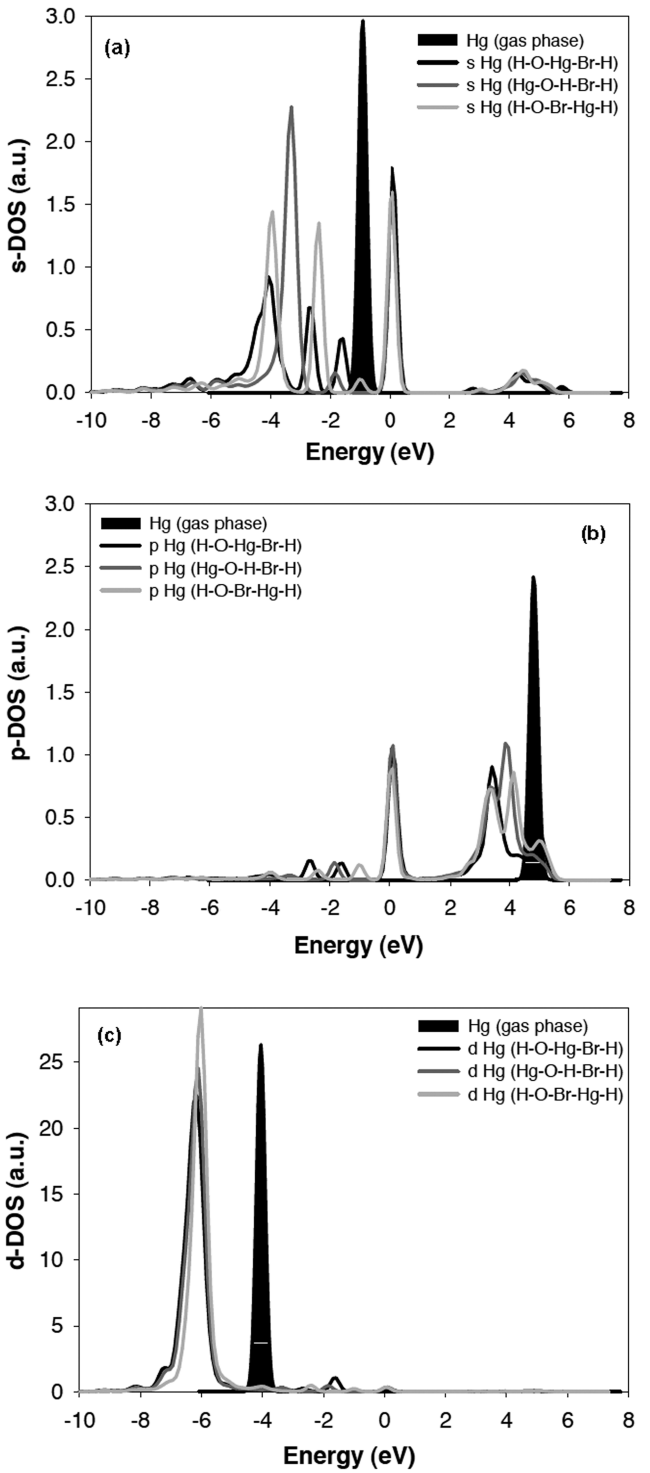


**Figure 5.** DOS showing the (a) s-, (b) p-, and (c) d-orbitals of Hg for various surface configurations compared with gas-phase $Hg^0$ shown in black.

at the surface. For instance, when Br neighbors Hg, two notable Hg s- and Br p-peaks form—one through this indirect surface modification and a second stronger (lower in energy) interaction through the direct Hg s- and Br p-orbitals. This splitting of the Hg s-electrons acts to reduce the strength of the Hg surface bond, making it less stable. Although the plots of both structures with the Hg-Br surface configuration (i.e., H-O-Hg-Br-H [Figure 6a] and H-O-Br-Hg-H [Figure 6c]) show the split Hg s- and Br p-peaks, the peaks are much stronger in the case of H-O-Br-Hg-H, in which O is not adjacent to Hg and thus does not detract from Hg's interaction with Br. On the other hand, as can be seen in the configuration of Figure 6b (Hg-O-H-Br-H, in which Br does not neighbor Hg), this interaction is not present, and the Hg s-peak corresponds primarily with O p-states. This Hg-O-H-Br-H configuration is the most stable structure of those simulated, likely because there is no direct Hg-Br interaction to destabilize the Hg-C bond.

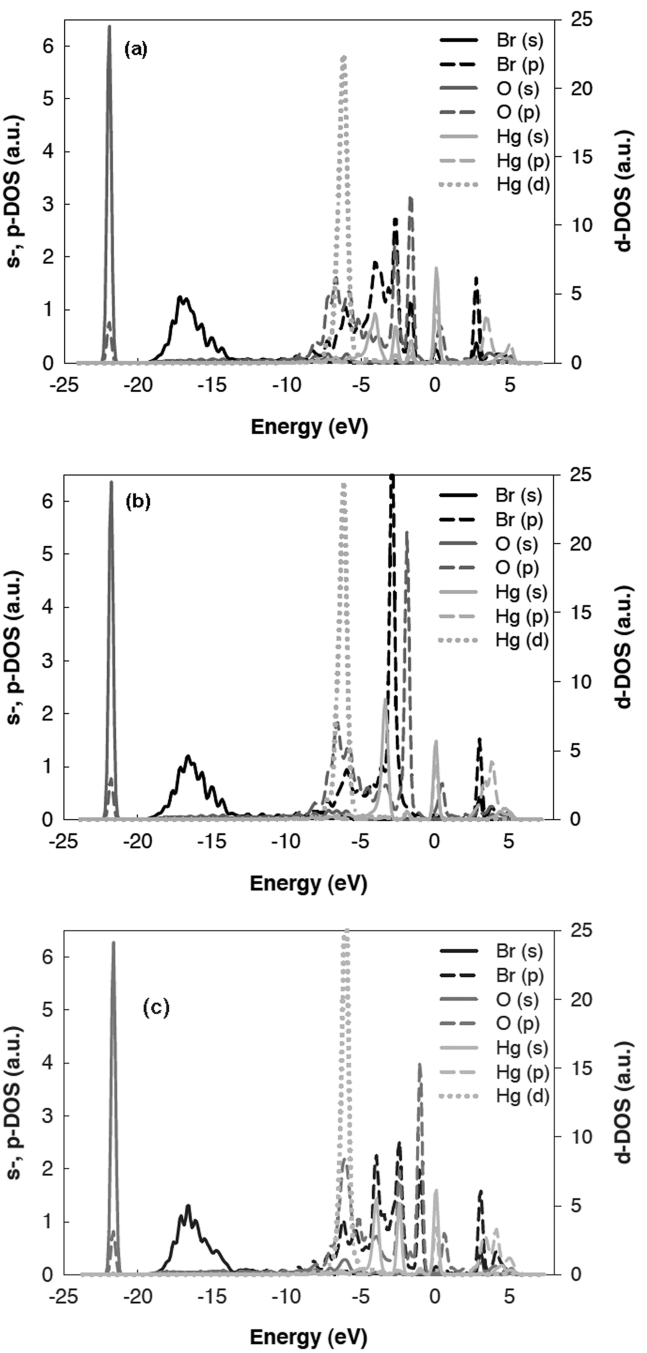


**Figure 6.** DOS showing the s-, p- (left axis), and d- (right axis) orbitals of surface atoms for (a) H-O-Hg-Br-H, (b) Hg-O-H-Br-H, and (c) H-O-Br-Hg-H.

To date, only a small sample of all of the possible configurations of Br, O, H, and Hg on the model AC surfaces has been investigated. Even with this small sample it is possible to gain some insight into the mechanism by which Hg is interacting with the surface. The strength of the Hg-graphene interaction is very sensitive to the local environment. In particular, the Hg binding energy strengthens when the Hg is located next to a surface O but not immediately next to a bound Br atom. Through the DOS analysis, it appears that Br modifies the electron density of the surface C, making the Hg-C bond weaker. In each of these cases investigated, configurations including direct Hg-C bonding with neighboring oxidizing atoms are presented; however, future work should include adsorbed configurations of Hg-Br and/or Hg-O to determine whether there are steps involving oxidation, desorption, and readsorption of the $Hg^{1+}$ oxidized form of Hg (i.e., HgBr) to become fully oxidized on the surface through a combination of a neighboring oxidizing atom (Br or O) or C.

## SUMMARY

Through XPS surface characterization studies, it was found that $Hg^0$ is most likely oxidized via Br, resulting in a surface-bound oxidized Hg species, but that O cannot be ruled out as a possible contributor in the oxidation/adsorption processes. Additionally, preliminary theoretical results indicate that the position of certain surface atoms plays a role in stabilizing Hg on the surface. The Hg-C interaction is strongest when Br is a next-nearest neighbor and O is a nearest neighbor, resulting in the overall tighter Hg-C binding. The results suggest that the C surface can be tuned to serve as an ideal sorbent because Br and O can serve to tightly bind Hg in a surface-bound oxidized form.

## ACKNOWLEDGMENTS

The authors acknowledge the financial support of the Electric Power Research Institute (EPRI). Valuable discussions with Thomas F. Jaramillo, Arindom Saha, and David Abram are gratefully acknowledged. The computations were carried out on the Center for Computational Earth & Environmental Science (CEES) cluster at Stanford University.

## REFERENCES

1. Cianciola, M.E.; Echeverria, D.; Martin, M.D.; Aposian, H.V.; Woods, J.S. Epidemiologic Assessment of Measures Used to Indicate Low-Level Exposure to Mercury Vapor (Hg); *J. Toxicol. Environ. Health* **1997**, *52*, 19-23.
2. Ngim, C.H.; Foo, S.C.; Boey, K.W.; Jeyaratnam, J. Chronic Neurobehavioural Effects of Elemental Mercury in Dentists; *Br. J. Ind. Med.* **1992**, *49*, 782-790.
3. Shapiro, J.M.; Cornblath, D.R.; Summer, A.J.; Uzzell, B.; Spitz, L.K.; Ship, I.L. Neurophysiological and Neuropsychological Function in Mercury-Exposed Dentists; *Lancet*, **1982**, *1*, 1147-1150.
4. Uzzell, B.P.; Oler, J. Chronic Low-Level Mercury Exposure and Neuropsychological Functioning; *J. Clin. Exp. Neuropsychol.* **1986**, *8*, 581-593.
5. Echeverria, D.; Heyer, N.J.; Martin, M.D.; Naleway, C.A.; Woods, J.S.; Bittner, A.C. Behavioral Effects of Low-Level Exposure to Hg among Dentists; *Neurotoxicol. Teratol.* **1995**, *17*, 161-168.
6. Nilsson, B.; Gerhardsson, L.; Nordberg, G.F. Urine Mercury Levels and Associated Symptoms in Dental Personnel; *Sci. Total Environ.* **1990**, *94*, 179-185.
7. Ritchie, K.A.; Gilmour, W.H.; Macdonald, E.B.; Burke, F.J.; McGowan, D.A.; Dale, I.M. Health and Neuropsychological Functioning of Dentists Exposed to Mercury; *Occup. Environ. Med.* **2002**, *59*, 287-293.
8. Rohling, M.I.; Demakis, G.J. A Meta-Analysis of the Neuropsychological Effects of Occupational Exposure to Mercury; *Clin. Neuropsychol.* **2006**, *20*, 108-132.
9. Hilt, B.; Svendsen, K.; Syversen, T.; Aas, O.; Qvenild, T.; Sletvold, H.; Melo, I. Occurrence of Cognitive Symptoms in Dental Assistants with Previous Occupational Exposure to Metallic Mercury; *Neurotoxicology* **2009**, *30*, 1202-1206.
10. Clarkson, T.W.; Magos, L. The Toxicology of Mercury and Its Chemical Compounds; *Crit. Rev. Toxicol.* **2006**, *36*, 609-662.
11. Chen, W.-C.; Lin, H.-Y.; Yuan, C.-S.; Hung, C.-H. Kinetic Modeling on the Adsorption of Vapor-Phase Mercury Chloride on Activated Carbon by Thermogravimetric Analysis; *J. Air & Waste Manage. Assoc.* **2009**, *59*, 227-235; doi: 10.3155/1047-3289.59.2.227.
12. Lee, C.W.; Serre, S.D.; Zhao, Y.; Lee, S.J.; Hastings, T.W. Mercury Oxidation Promoted by a Selective Catalytic Reduction Catalyst under Simulated Powder River Basin Coal Combustion Conditions; *J. Air & Waste Manage. Assoc.* **2008**, *58*, 484-493; doi: 10.3155/1047-3289.58.4.484.
13. Huggins, F.E.; Yap, N.; Huffman, G.P.; Senior, C.L. XAFS Characterization of Mercury Captured from Combustion Gases on Sorbents at Low Temperatures; *Fuel Process. Technol.* **2003**, *82*, 167-196.
14. Hutson, N.D.; Attwood, B.C.; Scheckel, K.G. XAS and XPS Characterization of Mercury Binding on Brominated Activated Carbon; *Environ. Sci. Technol.* **2007**, *41*, 1747-1752.
15. Laumb, J.D.; Benson, S.A.; Olson, E. S. X-Ray Photoelectron Spectroscopy Analysis of Mercury Sorbent Surface Chemistry; *Fuel Process. Technol.* **2004**, *85*, 577-585.
16. Weinberg, W.H. *Dynamics of Gas-Surface Interactions*; Rettner, C.T., Ashford, M.N.R., Eds.; Royal Society of Chemistry: Cambridge, United Kingdom, 1991; pp 171.
17. Rettner, C.T.; Aurbach, D.J. Distinguishing the Direct and Indirect Products of a Gas-Surface Reaction; *Science* **1994**, *263*, 365-367.
18. Rettner, C.T. Reaction of an H-atom Beam with Cl/Au(111): Dynamics of Concurrent Eley-Rideal and Langmuir-Hinshelwood Mechanisms; *J. Chem. Phys.* **1994**, *101*, 1529-1546.
19. Cheng, C.C.; Lucas, S.R.; Gutleben, H.; Choyke, W.J.; Yates, J.T., Jr. Atomic Hydrogen-Driven Halogen Extraction from Silicon (100): Eley-Rideal Surface Kinetics; *J. Am. Chem. Soc.* **1992**, *114*, 1249-1252.
20. Kresse, G.; Hafner, J. Ab Initio Molecular Dynamics for Open-Shell Transition Metals; *Phys. Rev. B.* **1993**, *48*, 13115-13118.
21. Kresse, G.; Furthmuller, J. Efficiency of Ab-Initio Total Energy Calculations for Metals and Semiconductors Using a Plane-Wave Basis Set; *Comput. Mater. Sci.* **1996**, *6*, 15-50.
22. Blöchl, P.E. Projector Augmented-Wave Method; *Phys. Rev. B.* **1994**, *50*, 17953-17979.
23. Kresse, G.; Joubert, D. From Ultrasoft Pseudopotentials to the Projector Augmented-Wave Method; *Phys. Rev. B.* **1999**, *59*, 1758-1775.
24. Perdew, J.P.; Burke, K.; Ernzerhof, M. Generalized Gradient Approximation Made Simple; *Phys. Rev. Lett.* **1996**, *77*, 3865-3868.
25. Methfessel, M.; Paxton, A.T. High-Precision Sampling for Brillouin-Zone Integration in Metals; *Phys. Rev. B.* **1989**, *40*, 3616-3621.
26. Monkhorst, H.J.; Pack, J.D. Special Points for Brillouin-Zone Integrations; *Phys. Rev. B.* **1976**, *13*, 5188-5192.
27. Briggs, D.; Seah, M.P. *Practical Surface Analysis (Appendix 5)*; John Wiley & Sons: New York, 1996.
28. Radovic, L.R.; Bockrath, B. The Mechanism of $CO_2$ Chemisorption on Zigzag Carbon Active Sites: a Computational Chemistry Study; *Carbon* **2005**, *43*, 907-915.
29. Padak, B.; Wilcox, J. Understanding Mercury Binding on Activated Carbon; *Carbon* **2009**, *47*, 2855-2864.
30. Radovic, L.R.; Bockrath, B. On the Chemical Nature of Graphene Edges: Origin of Stability and Potential for Magnetism in Carbon Materials; *J. Am. Chem. Soc.* **2005**, *127*, 5917-5927.
31. Yang, F.H.; Yang, R.T. Ab Initio Molecular Orbital Study of Adsorption of Atomic Hydrogen on Graphite: Insight into Hydrogen Storage in Carbon Nanotubes; *Carbon* **2002**, *40*, 437-444.
32. Chen, N.; Yang, R.T. Ab Initio Molecular Orbital Study of the Unified Mechanism and Pathways for Gas-Carbon Reactions; *J. Phys. Chem. A.* **1998**, *102*, 31, 6348-6356.
33. Stein, S.E.; Brown, R.L. Chemical Theory of Graphite-Like Molecules; *Carbon* **1985**, *23*, 105-109.
34. Padak, B.; Wilcox, J. Mercury Binding on Activated Carbon; *Environ. Prog.* **2006**, *25*, 319-326.
35. Zhu, Z.H.; Radovic, L.R.; Lu, G.Q.; Wu, X.X. *Computational Chemistry of Zigzag and Armchair Sites in Carbon Oxidation*. Presented at the 25th Biennial Conference on Carbon, Lexington, KY, 2001.
36. Olson, E.S.; Laumb, J.D.; Benson, S.A.; Dunham, G.E.; Sharma, R.K.; Mibeck, B.A.; Miller, S.J.; Holmes, M.J.; Pavlish, J.H. Chemical Mechanisms in Mercury Emission Control Technologies; *J. Phys. IV France* **2003**, *107*, 979-982.
37. Huggins, F.E.; Huffman, G.P.; Dunham, G.E.; Senior, C.L. XAFS Examination of Mercury Sorption on Three Activated Carbons; *Energy Fuels* **1998**, *13*, 114-121.

38. Radovic, L.R.; Bockrath, B. What (Exactly) Is on the Edge of a Graphene Sheet? Presented at the International Conference Nanocarbons, Nagano, Japan, 2001.
39. Olson, E.S.; Laumb, J.D.; Benson, S.A.; Dunham, G.E.; Sharma, R.K.; Mibeck, B.A.; Miller, S.J. An Improved Model for Flue Gas-Mercury Interactions on Activated Carbons. In *Proceedings of a Mega Symposium and A&WMA's Specialty Conference*; A&WMA: Pittsburgh, PA, 2003.
40. Desch, C.H. *The Chemistry of Solids*; Cornell University: Ithaca, NY, 1934.
41. Harrison, W.A. *Electronic Structure and the Properties of Solids: the Physics of the Chemical Bond*; Freeman: San Francisco, 1980.
42. Bandosz, T.J.; Ania, C.O. Surface Chemistry of Activated Carbons and Its Characterization; In *Activated Carbon Surfaces in Environmental Remediation*; Elsevier: Oxford, United Kingdom, 2006; pp 159-229.
43. Cecconi, F.; Ghilardi, C.A.; Midollini, S.; Orlandini, A.; Vacca, A. Synthesis, Characterization and X-Ray Structure of the Organomercurial Complex $Hg(C_6F_5)(NP_3)](CF_3SO_3)$, $NP_3=N(CH_2CH_2PPh_2)_3$; *Polyhedron*, **2001**, *20*, 2885-2888.
44. Borovik, A.S.; Bott, S.G.; Barron, A.R. Hydrogen/Deuterium Exchange Catalyzed by an Unusually Stable Mercury-Toluene Complex ; *Angew. Chem. Int. Ed.* **2000**, *39*, 4117-4118.

**About the Author**

Jennifer Wilcox is an assistant professor from Stanford University in the School of Earth Sciences and in the Energy Resources Engineering Department. Erdem Sasmaz and Abby Kirchofer are both Ph.D. students also at Stanford in the School of Earth Sciences in the Energy Resources Engineering and Earth, Energy, and Environmental Sciences Departments, respectively. Sang-Sup Lee is an assistant professor in the Department of Environmental Engineering at Chungbuk National University in Cheongju, South Korea. Please address correspondence to: Jennifer Wilcox, Department of Energy Resources Engineering, School of Earth Sciences, Stanford University, Green Earth Sciences 065, 367 Panama Street, Stanford, CA 94305; phone: +1-650-724-9449; fax: +1-650-725-2099; e-mail: wilcoxj@stanford.edu.